Cellular memory in eukaryotic chemotaxis depends on the background chemoattractant concentration

Richa Karmakar, Man-Ho Tang, Haicen Yue, Daniel Lombardo, Aravind Karanam, Brian A. Camley, Alex Groisman, and Wouter-Jan Rappel¹,

¹Department of Physics, University of California, San Diego, La Jolla, California 92093, USA
²Courant Institute for Mathematical Sciences, New York University, New York, New York 10012, USA
³Department of Physics & Astronomy, Department of Biophysics, Johns Hopkins University

Cells of the social amoeba *Dictyostelium discoideum* migrate to a source of periodic traveling waves of chemoattractant as part of a self-organized aggregation process. An important part of this process is cellular memory, which enables cells to respond to the front of the wave and ignore the downward gradient in the back of the wave. During this aggregation, the background concentration of the chemoattractant gradually rises. In our microfluidic experiments, we exogenously applied periodic waves of chemoattractant with various background levels. Surprisingly, we find that increasing background does not make detection of the wave more difficult, as would be naively expected. Instead, we see that the chemotactic efficiency significantly increases for intermediate values of the background concentration but decreases to almost zero for large values in a switch-like manner. These results are consistent with a computational model that contains a bistable memory module, along with a non-adaptive component. Within this model, an intermediate background level helps preserve directed migration by keeping the memory activated, but when the background level is higher, the directional stimulus from the wave is no longer sufficient to activate the bistable memory, suppressing directed migration. These results suggest that raising levels of chemoattractant background may facilitate the self-organized aggregation in *Dictyostelium* colonies.

Keywords: Dictyostelium discoideum, chemotaxis, cell migration, bistability

Chemotaxis, the movement of cells guided by chemical gradients, plays an important role in many biological processes including tumor dissemination, wound healing, and embryogenesis [1-4]. One of the most studied chemotaxis model organisms is the social amoeba *Dictyostelium discoideum*. Following starvation, *Dictyostelium* cells secrete a chemoattractant, cAMP, in a periodic fashion [5]. This chemoattractant signal is relayed by neighboring cells resulting in waves that sweep over the cell population with periods that range from 6-10 minutes [5-7]. These waves spontaneously organize themselves in spiral or target waves, leading to large-scale patters of cell migration and eventually generating aggregation centers that attract tens of thousands of cells. Within the resulting aggregates, cells differentiate, with the majority turning into spore cells.

Multiple aspects of this biological system have been investigated using computational and mathematical modeling . Models have addressed instabilities responsible for large scale migration patterns [9] [0], the coupling between

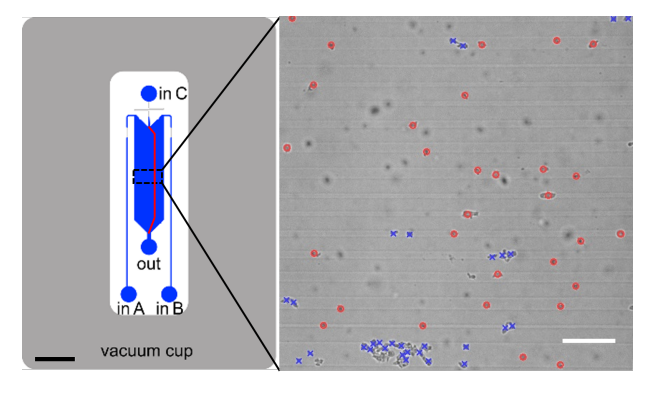


FIG. 1: Left: Schematic of the microfluidic wave device, with observation region indicated by black box (Scale bar: 3 mm). Right: Snapshot of cells moving on the micropatterned substrate, with symbols corresponding to cells identified by the machine learning algorithm (red circles: cells used in our analysis; blue X's: excluded cells that are too close to one another; scale bar: $100 \ \mu m$).

^{*}Electronic address: rappel@physics.ucsd.edu

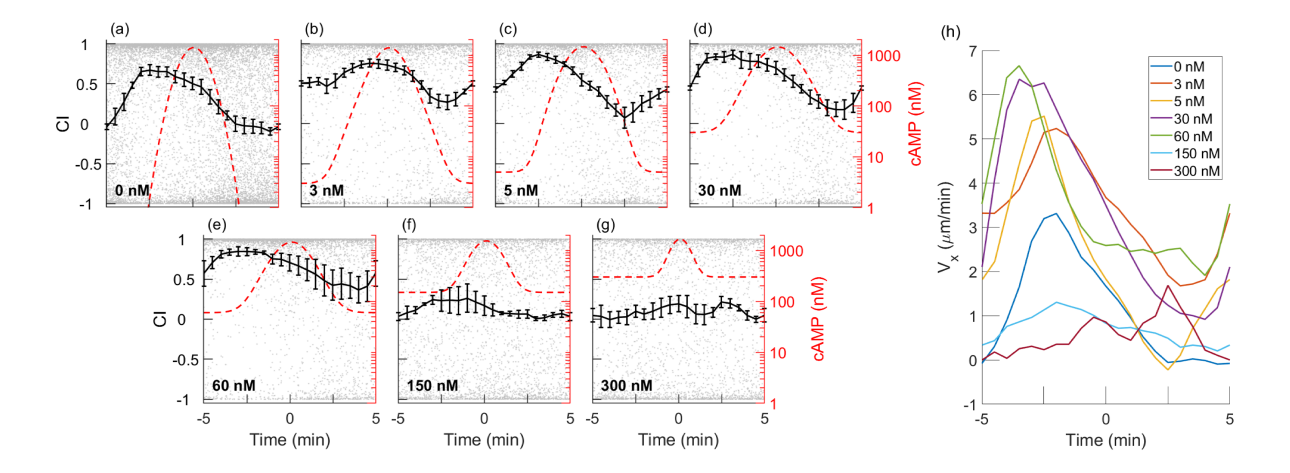


FIG. 2: (a-g) Experimentally determined average CI as a function of time (measured relative to peak of wave) for different concentrations of background cAMP (0-300nM). In each panel, gray dots represent the CI of individual cells, the black curve is the binned average over N=3-4 different experiments, and the dotted red line is the cAMP concentration of the wave. (h) Average x-component of the velocity of cells for different concentration of background cAMP. Time is binned in intervals of 0.5 min.

intracellular signaling and morphological changes [11-13], and the topology of signaling pathways responsible for guided motion [14-16]. Furthermore, models have addressed potential mechanisms of gradient sensing [8] [17] while a number of studies have examined the role of noise in the chemotactic response [18-20].

Recently, several experimental and modeling studies have also addressed the so-called back-of-the-wave problem in the chemotactic response to traveling waves [21]-23]. If cells respond only to spatial gradients, they would move forward in the front and backward in the back of the traveling wave, preventing aggregation. These studies have shown that cells exhibit memory, responding directionally to the front but not the back of the wave, enabling them to move efficiently toward the wave source [22] [23]. For wave periods shorter than 10 min, this memory completely prevented reversals of cell migration, whereas for longer periods, cells started reversing their migration direction in the back of the wave [23]. A mathematical model, consisting of an upstream adaptive module and a downstream bistable module, was able to explain the response of cells to periodic waves of chemoattractant [23]. Similar memory phenomena have also been reported in other biological systems, including chemotactic neutrophils [24] [25].

In the experimental studies of memory in Dictyostelium chemotaxis, the cAMP waves were applied exogenously, with the cAMP concentration reaching nearly zero in the troughs of the waves. In cAMP waves that are endogenously produced by starving populations of Dictyostelium, however, the background cAMP concentration, cAMP_{bg}, increases from cycle to cycle [26]. This increase occurs because secreted cAMP is not completely removed by phosphodiesterases (PDEs), enzymes that are responsible for the degradation of cAMP and that are also secreted by the cells [27]. Hence, the question how a non-zero cAMP_{bg} affects chemotaxis is relevant to the aggregation, sporulation, and survival of Dictyostelium. Naively, one would expect a decrease in the cell's ability to migrate towards the source of the wave since the fractional gradient across the cell body, and thus the signal-to-noise ratio, decreases for increasing cAMP_{bg}. Another possibility is that the cells fully adapt to cAMP_{bg}, rendering the ability of cells to respond to gradients independent of the background concentration [28].

To experimentally study this question, we used a modified version of the microfluidics device from Ref. [23] in which a traveling, bell-shaped wave of cAMP with a peak of 1000 nM periodically sweeps across a gradient channel at a constant speed (Fig. [1]) see Supplemental Materials and Fig. S1 for further details). This wave profile is similar to the one measured for natural waves of cAMP [29] [30]. Importantly, and in contrast to previous studies, the background concentration of cAMP was a variable parameter. Another major modification was that the glass substrate in the gradient channel was micropatterned with $\sim 1.5 \ \mu m$ thick stripes of cell adhesion-blocking polyethylene glycol (PEG) gel, limiting the adhesion and migration of Dictyostelium cells to $\sim 10 \ \mu m$ wide stripes of plain glass oriented in the x-direction, along the gradient and perpendicular to the flow (Fig. [1]) see [31] for a detailed description of these micropatterned substrates). As a result, cell migration was effectively one-dimensional (1D), either up or down the gradient (positive or negative x-direction), greatly facilitating the collection and analysis of data as compared to 2D chemotaxis on a standard glass substrate.

In our experiments, we exposed cells to repeated waves of cAMP and recorded their movement, excluding the first wave, with a frame rate of 15 s. Cells were tracked with a custom-made machine-learning algorithm detailed

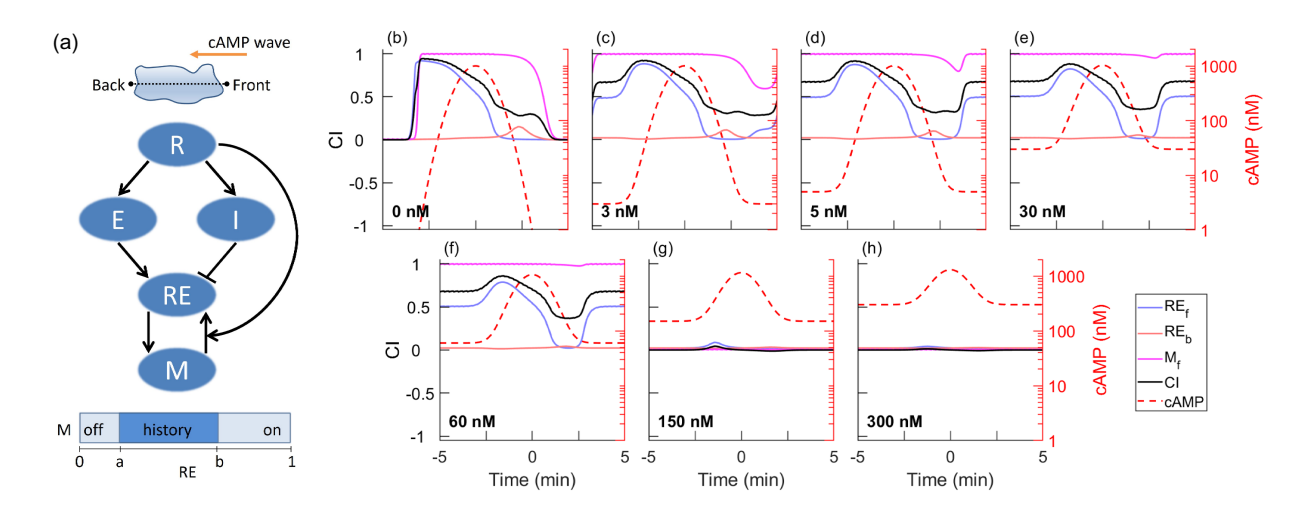


FIG. 3: (a) Schematic diagram of the chemotactic model, consisting of a receptor R, an activator E, an inhibitor I, a response element RE, and a memory component M. Simulations are carried out in a 1D geometry (top drawing). As indicated by the bottom bar, M is bistable, with a low and a high state, determined by parameters a and b. (b-h) Model results for different background cAMP concentrations added to a period wave, shown as a dashed red line. The black line represents the CI, the blue (red) line is the response RE at the front (back) of the cell, and the magenta line corresponds to the memory M at the front.

in Supplemental Materials, which was able to capture more than 90% of all cells. Only clearly isolated, single cells, marked by red circles in Fig. [1] were used in the analysis. Using cell tracks, we quantified the directional response by computing the chemotactic index CI, defined as ratio between the velocity in the x direction and the speed, computed as the difference in the x-position 3 frames prior and 3 frames forward: CI= V_x/V . This quantity ranges from +1 (cells with velocity perfectly aligned to the +x direction) and was computed by comparing cell locations 6 frames apart (for further details, see Supplemental Materials).

We first examined how cells responded to chemoattractant waves with a period of 10 minutes and zero background concentration. This wave period was chosen since it corresponds to the largest period for which the CI in 2D assays remained positive in the back of the wave [23]. The CI (black line in Fig. 2a), computed by averaging over different experiments and over 30s time-intervals, was nearly zero for cells ahead of the wave front, steeply increased to a maximum of ~ 0.7 as cells were exposed to the wave front, stayed high after the peak of the wave has passed, and gradually decayed to near zero but never became negative. This response is qualitatively similar to that in 2D Dictyostelium chemotaxis assays on plain substrates [23], indicating that constraining the cells to the narrow strips does not change their behavior and that the cellular memory reported in 2D assays is fully manifested in 1D assays as well.

Next, we exposed cells to the same periodic waves but with a non-zero cAMP_{bg} (Fig. 2b-g). Surprisingly, the average CI improved significantly for low values of cAMP_{bg}(cAMP_{bg}=3, 5, 30, and 60 nM). Most notably, for these values of cAMP_{bg}, the CI remained significantly greater than 0 during the entire wave cycle. Furthermore, the CI showed a clear minimum after the peak of the wave has passed and *increased* towards the end of the wave cycle even though cAMP was at its lowest level (Fig. 2b-e). For the two largest values of cAMP_{bg} tested, cAMP_{bg}=150 nM and 300 nM, the CI was significantly reduced and remained close to zero throughout the entire wave cycle (Fig. 2f-g). Thus, the background cAMP concentration has a profound effect on the chemotactic response, with intermediate/large values of cAMP_{bg} enhancing/suppressing the response.

The effect of the background concentration was also evident from the quantification of the x-component of the velocity, V_x . This quantification is shown in Fig. 2h where we plot V_x , also averaged over different experiments and over 30s time-intervals, as a function of time for different cAMP_{bg}. While this velocity component remained positive or close to zero during the entire cycle for all values of cAMP_{bg}, its maximum value is clearly larger for intermediate values of cAMP_{bg} than for cAMP_{bg}=0nM. Furthermore, V_x is significantly reduced for the two largest background concentrations tested (cAMP_{bg}=150 and 300 nM).

To investigate plausible mechanisms for this enhanced cellular memory, we turned to modeling. Specifically, we asked whether the cellular memory model developed by Skoge et al. [23] can reproduce the experimental results. This model describes the chemotaxis pathway in terms of abstract variables, although, for some, identification with biochemical components may be possible. Key features of this model are perfect adaptation upon uniform stimulation and cellular memory in gradients [23, 32]. It is schematically shown in Fig. [3] and contains an adaptive module, which

incorporates an incoherent feedforward Local Excitation Global Inhibition (LEGI) mechanism [14, 15] and consists of a receptor R, an activator E, an inhibitor I and a response element RE (Fig. [3a]). In addition, the model contains a memory module, which is assumed to be bistable such that its component M can be either in a low or high state. The transition between these state is determined by two thresholds, a and b (see also Supplemental Materials) and M feeds back to RE. Importantly, this feedback depends on R and this non-adaptive link may be thought of as representing parallel pathways for chemotaxis described in experimental studies [33]. For simplicity, we neglect the detailed morphology of the cell and model it as a 10 μ m line with the two endpoints representing the front and back, respectively (Fig. [3a]). At the front, the model is written as

$$\frac{dR_f}{dt} = k_R(\text{cAMP} + \text{cAMP}_{bg})(R_f^{tot} - R_f) - k_{-R}R_f$$
(1)

$$\frac{dE_f}{dt} = k_E R_f - k_{-E} E_f \tag{2}$$

$$\frac{dM_f}{dt} = -k_{Mem}M_f(M_f - M_f^{tot}) \left(M_f - M_f^{tot} \frac{b - RE_f}{b - a}\right)$$
(3)

$$\frac{dRE_f}{dt} = k_{RE}E_f \frac{RE_f^{tot} - RE_f}{K_{m1} + RE_f^{tot} - RE_f} - k_{-RE}I \frac{RE_f}{K_{m2} + RE_f} + k_{RE2}M_fR_f \frac{RE_f^{tot} - RE_f}{K_{m3} + RE_f^{tot} - RE_f}$$
(4)

and a similar set of equations applies for the components at the back, labeled with subscript b. The first equation describes the binding/unbinding dynamics of cAMP to the receptor with on and off rates k_R and k_{-R} , respectively. Here, cAMP is the time-varying concentration due to the wave and its dynamics is taken from a Gaussian fit to the wave profile (see Supplemental Materials). The second equation models the activator dynamics, parametrized by the activation rate k_E and the degradation rate k_{-E} . The third equation describes the bistable memory module, which has two stable steady states 0 and M_f^{tot} . The output of the model, RE, obeys Michaelis-Menten kinetics and is activated with rate k_{RE} by the activator E. It is de-activated with rate k_{-RE} by an inhibitor I, which diffuses within the interior of the cell. We will assume that I is uniform throughout the cell, corresponding to a high diffusion rate, and is activated by the average of R between the front and the back $R_{av} = (R_f + R_b)/2$, along with a small basal activity k_{basal} , and can spontaneously degrade with rate k_{-I} :

$$\frac{dI}{dt} = k_I(k_{basal} + R_{av}) - k_{-I}I\tag{5}$$

We set the Michaelis constants, K_{m1} and K_{m2} , to be small $(K_{m1}, K_{m2} \ll 1)$ to achieve near zero-order ultrasensitivity, which, consistent with experiments, can result in the amplification of shallow external cAMP gradient [34, 35]. The last term in the equation for RE_f describes the feedback from the memory module to the activation of RE_f , parametrized by the activation rate k_{RE2} and Michaelis constant K_{m3} . For simplicity, we will take $M_f^{tot} = M_b^{tot} = RE_f^{tot} = RE_b^{tot} = R_f^{tot} = R_b^{tot} = R_b^{tot}$

Model parameters were determined using a fitting procedure (detailed in Supplemental Materials), which minimized a loss function L that compared simulation results (x_{sim}) to experimental results (x_{exp}) with uncertainty σ_{exp} : $L = \sum_{n=1}^{N} |x_{exp} - x_{sim}|/(N\sigma_{exp})$. Here, N = 54 with 46 data points chosen from previous experiments [23] 32] and the remaining 8 data points chosen from the current experiments. Details of the previous data points used in the fitting are presented in Supplemental Materials while the new data points consisted of data for cAMP_{bg} of 0, 3, 60, and 150nM that were chosen since they represent the three qualitatively distinct responses observed in the experiments. Specifically, in our fitting we required that M_f 2.5 minutes before and 3 minutes after the peak to be either 0, corresponding to a small experimental value of CI, or 1, corresponding to a high CI in the experiments (see Supplemental Materials). Simulated annealing was used to find possible global minima, followed by a pattern search to obtain the local minima using the Matlab routine patternsearch. Importantly, the parameter values for the bistable and adaptive module were taken from previous studies and only parameters associated with the memory module (a, b, k_{Mem} , k_{RE2} and K_{m3}) were adjusted. The parameter values obtained by our fitting procedure are listed in Table S1 while a fit to previous data is shown in Fig. S2.

Simulation results for cAMP_{bg}=0 (Fig. 3b) show that the chemotactic response, quantified by CI (computed, following our earlier study 23, as a linear combination of RE and M: CI= $0.388(M_f - M_b) + 0.612(RE_f - RE_b)$) is in close agreement with the experimentally measured CI (cf. Fig. 2a). In this case, as the wave approaches the cell, the small difference in cAMP between the front and back is greatly amplified because of the ultra-sensitivity of the response. The resulting large increase in RE_f (blue line) causes a transition of M_f (magenta line) to the high state. Since RE_b (red line) remains low, M_b stays in the low state, and the CI is high (black line). After the wave sweeps over the cell, RE_f decreases while M_f remains high for several minutes, resulting in cellular memory and an elevated CI. Eventually, however, the low values of RE_f cause a transition of M_f to its low state and the CI decreases to zero (see Supplemental Materials and Fig. S3).

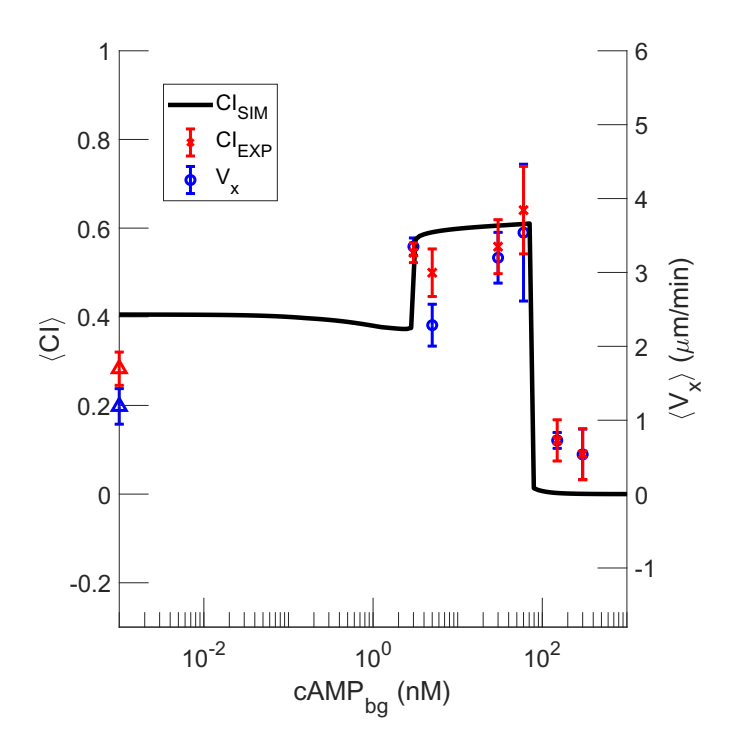


FIG. 4: Average CI (red symbols) and average V_x (blue symbols) versus background cAMP concentration.

Intermediate values of cAMP_{bg} (cAMP_{bg}=3-73 nM) result in higher values of RE_f , maintaining M_f in a high state for the entire wave period (Fig. 3c-f and Fig. S3). This increase in RE_f is due to the feedback from M_f to RE_f , which is, through the non-adaptive link, proportional to the receptor occupancy R_f . Since this occupancy is an increasing function of cAMP_{bg}, the feedback loop between RE_f and M_f contributes to a sustained positive CI throughout the entire wave cycle (Fig. 3c-f), in agreement with the experimental results. This feedback from high M_f is also responsible for the increase of RE_f in the back of the wave (Fig. 3c-f). As a result, the CI shows a distinct increase near the end of a cycle, which is, again, consistent with the experimental results.

For cAMP_{bg}>73 nM, both RE_f and CI remain close to 0 during the entire cycle, which is consistent with the experimental results for cAMP_{bg}=150 and 300 nM. The reason for this is that the amplification of RE_f due to the ultra-sensitivity of the response is reduced for increased values of cAMP_{bg} (see Supplemental Materials and Fig. S3). As a result, the value of RE_f is not sufficiently large to bring M_f to its high state. Consequently, M_f remains in the low state, leading to a short and weak response of RE_f and an overall low CI (Fig. 3g-h and Fig. S3). Note that for our parameter values, the dissociation constant for the receptors is $K_d \approx 408$ nM. Thus, the absence of a strong chemotactic response for high values of cAMP_{bg} is not due to receptor saturation but is directly linked to the bistability and the ultra-sensitivity of the pathway.

We also used the modeling results to compute the chemotactic index averaged in time over the entire wave cycle, $\langle \text{CI} \rangle$. The dependence of $\langle \text{CI} \rangle$ on cAMP_{bg} has three distinct regimes (Fig. 4). For very small values of cAMP_{bg} (cAMP_{bg}< 3 nM) $\langle \text{CI} \rangle$ remains close to its value at cAMP_{bg}=0. For these values of cAMP_{bg}, the memory is only turned on during part of the wave cycle. In contrast, for intermediate values of cAMP_{bg} (3 nM \leq cAMP_{bg} \leq 73 nM), M_f is in the high state during the entire cycle, resulting in a nearly constant and high $\langle \text{CI} \rangle$. Finally, for cAMP_{bg} > 73 nM, M_f is always in the low state and $\langle \text{CI} \rangle$ is close to 0. Notably, due to the bistable dynamics of our memory module, the transitions between these regimes are very abrupt and switch-like (Fig. S4).

To determine whether our experimental data also exhibited this switch-like behavior, we computed the average CI in the experiments. The results are plotted as red symbols in Fig. 4 and are close to the results of the model (line). Most importantly, CI decreases in a switch-like fashion from as much as ~ 0.6 at cAMP_{bg}=60nM to as little as ~ 0.15 at cAMP_{bg}=150nM, in agreement with the bistable dynamics of the memory module. A similar switch-like behavior can also be seen for the time averaged value of V_x , $\langle V_x \rangle$, plotted against cAMP_{bg} (blue symbols in Fig. 4).

In summary, we find that the background concentration of the chemoattractant, $cAMP_{bg}$, has a profound effect on the cellular memory of chemotaxing *Dictyostelium* cells. For intermediate values of $cAMP_{bg}$ this memory is greatly enhanced, leading to substantially more efficient chemotaxis under periodic waves of cAMP. It is worth noting that the experimentally estimated value of $cAMP_{bg}$ during the natural aggregation process of *Dictyostelium* cells is ~ 10 nM [26]. This value is within the intermediate range, suggesting that aggregation may be facilitated by increased cellular

memory due to accumulating cAMP. For larger values of $cAMP_{bg}$, the chemotactic response and cellular memory are suppressed. Our experimental results, and in particular the switch-like behavior of the average CI, are fully consistent with our mathematical model. Crucial elements of this model are a bistable memory module, which allows cells to ignore the back of the wave, an ultra-sensitive response, responsible for the amplification of the chemoattractant gradient, and a direct, non-adaptive link between input signal and response, which explains the long-lasting memory for intermediate values of $cAMP_{bg}$. Future work will be required to identify the precise biochemical components that are responsible for the observed behavior.

I. ACKNOWLEDGMENTS

R.K. and M-H.T. contributed equally to this work. We acknowledge support from by the National Science Foundation under grant NSF PHY-1915491 (BC), PHY-1411313 (AG), and PHY-1707637 (W.-J.R.).

- [1] Evanthia T Roussos, John S Condeelis, and Antonia Patsialou. Chemotaxis in cancer. Nature Reviews Cancer, 11(8):573, 2011.
- [2] Marco Baggiolini. Chemokines and leukocyte traffic. Nature, 392(6676):565, 1998.
- [3] Anne J Ridley, Martin A Schwartz, Keith Burridge, Richard A Firtel, Mark H Ginsberg, Gary Borisy, J Thomas Parsons, and Alan Rick Horwitz. Cell migration: integrating signals from front to back. *Science*, 302(5651):1704–1709, 2003.
- [4] Denise J Montell. Border-cell migration: the race is on. Nature Reviews Molecular Cell Biology, 4(1):13–24, 2003.
- [5] Thomas Gregor, Koichi Fujimoto, Noritaka Masaki, and Satoshi Sawai. The onset of collective behavior in social amoebae. Science, 328(5981):1021–1025, 2010.
- [6] W Roos, V Nanjundiah, D Malchow, and G Gerisch. Amplification of cyclic-amp signals in aggregating cells of dictyostelium discoideum. FEBS letters, 53(2):139–142, 1975.
- [7] BM Shaffer. Secretion of cyclic amp induced by cyclic amp in the cellular slime mould dictyostelium discoideum. *Nature*, 255(5509):549, 1975.
- [8] Herbert Levine and Wouter-Jan Rappel. The physics of eukaryotic chemotaxis. Phys Today, 66(2), Feb 2013.
- [9] Herbert Levine, Igor Aranson, Lev Tsimring, and Thai Viet Truong. Positive genetic feedback governs camp spiral wave formation in dictyostelium. *Proceedings of the National Academy of Sciences*, 93(13):6382–6386, 1996.
- [10] Giovanna De Palo, Darvin Yi, and Robert G Endres. A critical-like collective state leads to long-range cell communication in dictyostelium discoideum aggregation. *PLoS biology*, 15(4), 2017.
- [11] S. J. Shattil, C. Kim, and M. H. Ginsberg. The final steps of integrin activation: the end game. *Nat Rev Mol Cell Biol*, 11(4):288–300, 2010.
- [12] Danying Shao, Herbert Levine, and Wouter-Jan Rappel. Coupling actin flow, adhesion, and morphology in a computational cell motility model. *Proc Natl Acad Sci U S A*, 109(18):6851–6856, 2012.
- [13] Wieland Marth and Axel Voigt. Signaling networks and cell motility: a computational approach using a phase field description. *Journal of mathematical biology*, 69(1):91–112, 2014.
- [14] Carole A Parent and Peter N Devreotes. A cell's sense of direction. Science, 284(5415):765-770, 1999.
- [15] Andre Levchenko and Pablo A. Iglesias. Models of eukaryotic gradient sensing: application to chemotaxis of amoebae and neutrophils. *Biophys J*, 82:50–63, 2002.
- [16] Wouter-Jan Rappel and Herbert Levine. Receptor noise limitations on chemotactic sensing. PNAS, 105(49):19270–19275, 2008.
- [17] Pablo A. Iglesias and Peter N. Devreotes. Navigating through models of chemotaxis. Curr Opin Cell Biol, 20(1):35–40, 2008.
- [18] Wouter-Jan Rappel and Herbert Levine. Receptor noise and directional sensing in eukaryotic chemotaxis. *Physical review letters*, 100(22):228101, 2008.
- [19] Jose Negrete Jr, Alain Pumir, Hsin-Fang Hsu, Christian Westendorf, Marco Tarantola, Carsten Beta, and Eberhard Bodenschatz. Noisy oscillations in the actin cytoskeleton of chemotactic amoeba. *Physical review letters*, 117(14):148102, 2016.
- [20] Hsin-Fang Hsu, Eberhard Bodenschatz, Christian Westendorf, Azam Gholami, Alain Pumir, Marco Tarantola, and Carsten Beta. Variability and order in cytoskeletal dynamics of motile amoeboid cells. *Physical review letters*, 119(14):148101, 2017.
- [21] Raymond E Goldstein. Traveling-wave chemotaxis. Physical review letters, 77(4):775, 1996.
- [22] Akihiko Nakajima, Shuji Ishihara, Daisuke Imoto, and Satoshi Sawai. Rectified directional sensing in long-range cell migration. *Nature communications*, 5, 2014.
- [23] Monica Skoge, Haicen Yue, Michael Erickstad, Albert Bae, Herbert Levine, Alex Groisman, William F Loomis, and Wouter-Jan Rappel. Cellular memory in eukaryotic chemotaxis. *Proc Natl Acad Sci U S A*, 111(40):14448–53, Oct 2014.
- [24] Tim Lämmermann, Philippe V Afonso, Bastian R Angermann, Ji Ming Wang, Wolfgang Kastenmüller, Carole A Parent, and Ronald N Germain. Neutrophil swarms require ltb4 and integrins at sites of cell death in vivo. Nature, 498(7454):

- 371-375, 2013.
- [25] Bashar Hamza, Elisabeth Wong, Sachin Patel, Hansang Cho, Joseph Martel, and Daniel Irimia. Retrotaxis of human neutrophils during mechanical confinement inside microfluidic channels. *Integrative Biology*, 6(2):175–183, 2014.
- [26] KJ Tomchik and Peter N Devreotes. Adenosine 3', 5'-monophosphate waves in dictyostelium discoideum: a demonstration by isotope dilution—fluorography. *Science*, 212(4493):443–446, 1981.
- [27] Sonya Bader, Arjan Kortholt, and Peter JM Van Haastert. Seven dictyostelium discoideum phosphodiesterases degrade three pools of camp and cgmp. *Biochemical Journal*, 402(1):153–161, 2007.
- [28] Yuhai Tu and Wouter-Jan Rappel. Adaptation in living systems. Annual review of condensed matter physics, 9:183–205, 2018.
- [29] Peter N Devreotes, Michael J Potel, and Stephen A MacKay. Quantitative analysis of cyclic amp waves mediating aggregation in dictyostelium discoideum. *Developmental biology*, 96(2):405–415, 1983.
- [30] Marten Postma and Peter JM van Haastert. Mathematics of experimentally generated chemoattractant gradients. In *Chemotaxis*, pages 473–488. Springer, 2009.
- [31] Richa Karmakar, Christoph Schich, Nadine Kamprad, Vanessa Scheller, Edgar Gutierrez, Alex Groisman, Wouter-Jan Rappel, and Marco Tarantola. Novel micropatterning technique reveals dependence of cell-substrate adhesion and migration of social amoebas on parental strain, development, and fluorescent markers. *In review*, 2020.
- [32] Kosuke Takeda, Danying Shao, Micha Adler, Pascale G Charest, William F Loomis, Herbert Levine, Alex Groisman, Wouter-Jan Rappel, and Richard A Firtel. Incoherent feedforward control governs adaptation of activated ras in a eukary-otic chemotaxis pathway. Sci. Signal., 5(205):ra2, 2012.
- [33] L. Bosgraaf and P. J. Van Haastert. Navigation of chemotactic cells by parallel signaling to pseudopod persistence and orientation. PLoS ONE, 4(8):e6842, 2009.
- [34] Monica Skoge, Micha Adler, Alex Groisman, Herbert Levine, William F Loomis, and Wouter-Jan Rappel. Gradient sensing in defined chemotactic fields. *Integrative Biology*, 2(11-12):659–668, 2010.
- [35] Arpan Bhowmik, Wouter-Jan Rappel, and Herbert Levine. Excitable waves and direction-sensing in dictyostelium discoideum: steps towards a chemotaxis model. *Physical biology*, 13(1):016002, 2016.